NUMERICAL STUDY ON RESTRAINMENT OF REINFORCED CONCRETE DUE TO AAR EXPANSION

Mariana C. Posterlli[1], Rodolfo A. K. Sanches[1], Rodrigo R. Paccola[1], Rogério Carrazedo[1*]

[1]USP, University of São Paulo at São Carlos School of Engineering, São Carlos, SP, BRAZIL

Abstract

Alkali aggregate reaction leads to formation of a hygroscopic expansive gel, which may cause volumetric expansion of the concrete. In presence of compressive stresses, expansion is decreased in the compression direction; however, if compression is not equally applied over the three directions, the restrained expansion is transferred to a less compressed direction. In this sense, rebars reduce AAR strain in its direction, but barely affect the others.

This pathology may considerably reduce the life span of the structure, however, modelling of an AAR-damaged structure should forecast displacements and strains development, thus allowing maintenance and improving structural safety.

In this work, we perform a numerical study on the effect of passive stresses induced by AAR strains on the degradation of reinforced structures.

Keywords: reinforcement; reinforced concrete; stress effect; numerical modelling.

1 INTRODUCTION

Concrete is the most important and widely used construction material. Due to its low tensile strength, is usually associated with reinforcing steel rebars, and when correctly designed and executed, is economically competitive in many types of structures. However, even if correctly designed, concrete may fail due to several mechanisms. Among them, alkali-aggregate reaction (AAR) is a great concern, especially in hydraulic structures and other structures in contact with water, such as piers and foundations. The reaction known as alkali-silica reaction (ASR) promotes the formation of a hygroscopic gel that swells, leading to internal stresses, cracks and deformation of the concrete, followed by reduction of mechanical properties, such as Young's modulus and mechanical strength.

The ASR development has not yet been completely elucidated, yet it is known that some conditions are closely related to its rate and magnitude, such as alkali content in concrete pore fluid, temperature, pressure and humidity, as well as size, amount and reactivity of the aggregates. Due to limited understanding of the reaction mechanism, its complexity, heterogeneity and random distribution inside a structure, several models were proposed, with different approaches. An extensive review of the current trend to model the ASR is made by Pan *et al.* [1].

At micro scale, some theoretical models describe a representative volume element, a cell with a spherical aggregate surrounded by cement paste, addressing the problem by the ionic diffusion through the barrier created by the reaction gel [2-5]. On the other hand, the reaction rate in some models is found by the Arrhenius law [6-8].

At macro scale, some empirical models based on field and laboratory observations of the expansion due to ASR were developed, usually associating a chemical proposed kinetic and a mechanical model [9]. The chemical kinetic may be approached by the saturated porous media theory of Biot, in which two elastic materials, the AAR gel and the concrete skeleton, are modeled. The mechanical model is found either considering damage theory [10] or fracture mechanics [11,12].

The objective of this study is to employ a kinetic macro-level model composed by the parametric model proposed by Léger *et al.* [13] and Pappalardo Jr. *et al.* [14], and the kinetic law expressed by an exponential equation proposed by Carrazedo and Lacerda [15], based on the work of Pietruszczak [16]. Besides, this paper presents a numerical study on the restrainment developed by steel bars in reinforced concrete structures. This subject is seldom observed in articles, where only restrainment due stresses and constrainment are evaluated, as in [17,18].

* Correspondence to: rogcarrazedo@sc.usp.br

The presented AAR model has been implemented in a FEM formulation able to analyse composite materials, constituted by an elastic matrix reinforced and by long and short fibers, including curved ones, with ideal bonding. In this case, there is no slip between fiber and matrix. The fiber elements are introduced by kinematics relations only, ensuring bonding without increasing the number of degree of freedom [19-21]. The continuum is discretized by a solid isoparametric finite element adopting positions as nodal parameters, instead of displacements, allowing us to model large deformations, although not employed here [22,23]. Saint-Venant-Kirchhoff constitutive law has been adopted to model the material behaviour [24].

The paper is organized as follows. Section 2 describes the parametric model employed to evaluate the concrete expansion due the alkali-aggregate reaction. Section 3 briefly explain the solution process, and how the fibers contribute on the material properties, without increasing the number of degrees of freedom. Section 4 presents some numerical examples of the formulation. Conclusions are presented in section 5.

2 DESCRIPTION OF THE MODEL

Léger *et at.* proposed the CTMR parametric model, in which the concrete expansion due AAR may be found by a linear combination of the factors that affects the AAR, namely mineral reactivity, total amount of free alkaline ions, as well as humidity, temperature, stress state and porosity [13]. These factors are normalized by laws obtained by phenomenological approaches, related to the influence observed in real structures and laboratory assessment.

Instead of employing a linear function, Pappalardo Jr. *et al.* proposed that the combination of the influence factors should be attained by a constitutive kinetic equation, able to represent the stages usually observed in a typical expansion due to AAR [14].

Based on the work of Pietruszczak [16], Carrazedo and Lacerda proposed the following exponential kinetic equation [15]:

$$\varepsilon_{AAR} = H(t - t^p F_P)\varepsilon_{vol}^{max}\left[1 - e^{\frac{-(t-t^p F_P)}{A_1 F_T}}\right]\sqrt{F_C F_M} \tag{1}$$

where ε_{AAR} is the expansion (strain) due to AAR, H is the Heaviside function, ε_{vol}^{max} is the asymptotic free volumetric strain due to AAR, A_1 is the reactivity index, F_M, F_P, F_C and F_T are the normalized influence factors of moisture, porosity, confinement and temperature, respectively, and t^p is the time (age) it takes for the beginning of expansion development, right before cracking of the aggregate. In this sense, the presented model can be classified as a kinetic macro-level model, yet empirical.

Notice that this kinetics equation is closely related to the equation presented by Larive [25], which employs two exponential functions, as A_1 resemble the characteristic time and t^p the latency time. The advantage of Larive kinetic equation is that it is able to evaluate the first stage of AAR development, when very little expansion due to AAR is observed. Equation (1) is unable to represent this initial stage.

It is worth noticing that, according to Saouma *et al.* [2], the general form of an AAR expansion is made of four consecutive stages, being the first the nucleation, also known as induction stage, in which the concrete voids are being filled by the reaction products and very little expansion due to AAR is observed. Development of the reaction rim happen at this stage. The second phase is the development, when most of the voids around aggregate fills in and expansion develops by internal pressure. The third stage is the acceleration, usually put together with the development, in which the cement paste cracks and gel swells away from the aggregate. The last stage is the extinction, when expansion and crack propagation have slowed down, normally due depletion of reactive minerals.

Nevertheless, Eq. 1 was proposed to assimilate the influence of several factors that affects AAR, main reason for its adoption. So, instead of relying on the normalization laws to obtain the expected behaviour of each factor that affects AAR, it was proposed that the behaviour should be controlled by the constitutive kinetic equation, leading to linear normalization laws, as presented in Fig. 1.

It is known that temperature affects the reaction rate, as stated by Arrhenius law. Yet, temperature has no influence on the final expansion amount. Instead of using temperature itself in Eq. 1, its influence is considered by the normalized factor F_T.

Regarding humidity, it is known that it is essential for gel formation and mobility within the structure. The normalized factor F_M allows us to forbid or to greatly reduce any expansion if moisture is under a threshold value. Eq. 1 simulates the non-linear behavior, fed by a hygroscopicity analysis.

Porosity plays another important role in the process, yet controversial. We assume that if the pore solution is filled by water, gel will took its place and start expanding. If the pore is not filled, it will take longer to fulfil and expand. So higher humidity values leads to earlier expansions. It is a crude assumption, as seen in [26], but this simplification may be used as a start for aging structures.

Regarding stress state, Multon and Toutlemonde have shown that volumetric expansion developed by AAR is constant, whichever imposed stress state or restraint [27]. When subjected to a compressive stress state or restraint in a direction, expansion is reduced along this direction, as in the case of reinforced concrete elements. Expansion is then transferred to a less compressed direction. The present model is not able to consider this expansion transfer so far, but the orthotropic behaviour is correctly observed [28].

Notice that these linear laws are governed by constants (k_m, k_p, k_c and k_t), that must be adjusted according to the problem to be solved. In addition, the boundaries presented in Fig. 1 were adopted, and stated only for guidance.

3 SOLUTION PROCESS

The total potential energy for the fiber reinforced mechanical problem is given by [21]:

$$\Pi = \int_{V_0} \Psi(E) dV_0 + \int_{V_0} \mathrm{u}_e(\boldsymbol{E}) dV_0 - \oint_{A_0} p \cdot y dA_0 - \boldsymbol{F} \cdot \boldsymbol{Y} \tag{2}$$

where Ψ is the Helmholtz free energy potential of elastic fibers, function of the uniaxial Green-Lagrange strain measured at fibers $(\boldsymbol{E})$, u_e is the specific strain energy potential of the elastic matrix, function of the Green-Lagrange strain developed at the elastic matrix $(\boldsymbol{E})$, $\boldsymbol{F}$ is the load vector related to position vector $(\boldsymbol{Y})$, and p is the distributed load related to the surface position (y).

The principle of stationary states that any variation of a conservative system is zero at equilibrium position. If the variation is assumed to be the nodal position vector, then

$$\delta\Pi = \int_{V_0} \frac{\partial \Psi}{\partial \boldsymbol{Y}} dV_0 \cdot \partial \boldsymbol{Y} + \int_{V_0} \frac{\partial u_e}{\partial \boldsymbol{Y}} dV_0 \cdot \partial \boldsymbol{Y} - \oint_{A_0} P \cdot \partial \boldsymbol{Y} dA_0 - \boldsymbol{F} \cdot \partial \boldsymbol{Y} = 0 \tag{3}$$

Assuming the energy conjugate assumption [29] and developing the first and second terms by means of the Green-Lagrange strain tensor, Eq. (3) is written as

$$\delta\Pi = \left(\int_{V_0} S \frac{\partial E}{\partial \boldsymbol{Y}} dV_0 + \int_{V_0} \boldsymbol{S} : \frac{\partial \boldsymbol{E}}{\partial \boldsymbol{Y}} dV_0 - \oint_{A_0} P dA_0 - \boldsymbol{F} \right) \cdot \partial \boldsymbol{Y} = 0 \tag{4}$$

The nonlinear equation must hold for any $\partial\mathbf{Y}$, and may be written as an unbalanced vector $\boldsymbol{\Delta F}$ for Newton-Raphson solution process, given by

$$\boldsymbol{\Delta F}(\boldsymbol{Y}) = \left(\int_{V_0} S \frac{\partial E}{\partial \boldsymbol{Y}} dV_0 + \int_{V_0} \boldsymbol{S} : \frac{\partial \boldsymbol{E}}{\partial \boldsymbol{Y}} dV_0 - \boldsymbol{M} \cdot \boldsymbol{P} - \boldsymbol{F} \right) = 0 \tag{5}$$

Eq. 6 may be expanded in Taylor series over a trial position $\boldsymbol{Y_{i-1}}$, as

$$\boldsymbol{\Delta F}(\boldsymbol{Y}) \cong \boldsymbol{\Delta F}(\boldsymbol{Y_{i-1}}) + \left. \frac{\boldsymbol{\partial \Delta F}}{\boldsymbol{\partial Y}} \right|_{\boldsymbol{Y_{i-1}}} \boldsymbol{\Delta Y} = \boldsymbol{0} \tag{6}$$

Solving the system given by Eq. 6, one finds a correction to the current position, applied until convergence or a tolerance is achieved. The derivative of the unbalanced vector results the Hessian matrix as

$$\frac{\boldsymbol{\partial \Delta F}}{\boldsymbol{\partial Y}} = \boldsymbol{H} = \left(\frac{\boldsymbol{\partial E}}{\boldsymbol{\partial Y}} \frac{\boldsymbol{\partial^2 \Psi}}{\boldsymbol{\partial E^2}} \frac{\boldsymbol{\partial E}}{\boldsymbol{\partial Y}} + \boldsymbol{S} \frac{\boldsymbol{\partial^2 E}}{\boldsymbol{\partial Y \partial Y}} \right) + \left(\frac{\boldsymbol{\partial E}}{\boldsymbol{\partial Y}} : \frac{\boldsymbol{\partial^2 u_e}}{\boldsymbol{\partial E \partial E}} : \frac{\boldsymbol{\partial E}}{\boldsymbol{\partial Y}} + \boldsymbol{S} : \frac{\boldsymbol{\partial^2 E}}{\boldsymbol{\partial Y \partial Y}} \right) \tag{7}$$

It is assumed that there is no slipping between fibers and the concrete matrix. In this case, it is possible to write the fibers degree of freedom as a function of the matrix degree of freedom. To do so, consider that the internal energy of a reinforced body is the sum of the internal energy of the concrete matrix and the reinforcement rebars. If the position vector of the discrete matrix at node β following direction α is given by Y_α^β and the position vector of the discrete rebar element at node P following direction i is given by Y_i^k, then the variation of the internal energy may be written as

$$\frac{\partial(\Psi + u_e)}{\partial Y_\alpha^\beta} = \frac{\partial u_e}{\partial Y_\alpha^\beta} + \frac{\partial \Psi}{\partial Y_\alpha^\beta} = \frac{\partial u_e}{\partial Y_\alpha^\beta} + \frac{\partial \Psi}{\partial Y_i^P}\frac{\partial Y_i^P}{\partial Y_\alpha^\beta} \tag{8}$$

No sum over P is implied. The same can be done for the second derivative, leading to

$$\frac{\partial^2(\Psi + u_e)}{\partial Y_\alpha^\beta \partial Y_\gamma^\xi} = \frac{\partial^2 u_e}{\partial Y_\alpha^\beta \partial Y_\gamma^\xi} + \frac{\partial^2 \Psi}{\partial Y_\alpha^\beta \partial Y_\gamma^\xi} \tag{9}$$

Appling chain rule twice in the second member of Eq. (9) results

$$\frac{\partial^2 \Psi}{\partial Y_\alpha^\beta \partial Y_\gamma^\xi} = \frac{\partial^2 \Psi}{\partial Y_i^P \partial Y_i^P}\frac{\partial Y_i^P}{\partial Y_\alpha^\beta}\frac{\partial Y_i^P}{\partial Y_\gamma^\xi} + \frac{\partial^2 \Psi}{\partial Y_i^P \partial Y_j^P}\frac{\partial Y_i^P}{\partial Y_\alpha^\beta}\frac{\partial Y_j^P}{\partial Y_\gamma^\xi} + \frac{\partial^2 \Psi}{\partial Y_j^P \partial Y_i^P}\frac{\partial Y_j^P}{\partial Y_\alpha^\beta}\frac{\partial Y_i^P}{\partial Y_\gamma^\xi} + \frac{\partial^2 \Psi}{\partial Y_j^P \partial Y_j^P}\frac{\partial Y_j^P}{\partial Y_\alpha^\beta}\frac{\partial Y_j^P}{\partial Y_\gamma^\xi} \tag{10}$$

Further development is out of topic, and can be found in [19-23], as well in [30,31]. Validation of this formulation has been exhaustively done, and may be seen in the aforementioned papers. Notice that, as only small and moderately small strains are allowed, one may additively decompose the Green-Lagrange strain:

$$\boldsymbol{E} = \boldsymbol{E_e} + \boldsymbol{\varepsilon_{AAR}} \tag{11}$$

where E_e is the elastic part of the strain and ε_{AAR} is the strain developed by AAR. This is considered henceforth.

4 EXAMPLES

4.1 Evaluation of different boundary conditions

In this example, we modeled two specimens evaluated by [18] to validate the effect of applied stresses in the present numerical model. The specimens consist of cylindrical specimens of 130 mm in diameter and 240 mm of height with strains measured for 450 days, one under free expansion and another applied loading of 10 MPa in the direction of the axis of the cylinder.

The following properties were adopted for concrete: Young's modulus of 37.3 GPa [18], asymptotic volumetric strain (ε_{vol}^{max}) of 0.1589, reactivity index (A_1) of 1411.05 days, porous filling time (t^p) of 30 days. The properties related to the presented model were calibrated to best fit the experimental results.

Besides, since the specimens were kept sealed under a watertight cover, the calibration variables related to moisture and porosity (k_m and k_p) were assumed equal unity (no influence). The calibration variable related to temperature (k_t) relates experimental and field measurements, since in controlled situations like laboratories the specimens have the reaction accelerated by increase of temperature. We employed a value of 0.2, which means that the specimen under temperature of 38°C have its reactions accelerated by 5.

The calibration variable related to stress state (k_c) was set equal to 0.001. In this case, if a principal stress is over -12MPa (an adopted limit) and according to Fig 1c, the expansion is reduced around 30 times compared to free expansion in that direction. Notice that damage and creep were not yet implemented, as is should, although both play important roles in the process.

Fig. 2 shows the discretization of the specimen into 466 20-node tetrahedral elements, employing 2612 nodes. No symmetry condition was employed. One may notice the good proximity between numerical and experimental results in Fig. 3. Notice that we consider that the expansion due only to AAR if found by the difference of the expansion of a reactive and a non-reactive (inert aggregate) specimen. That way we remove most of the expansion due creep and shrinkage, for example, from an AAR expansion curve. This concept follows the analysis of [32].

From this example we conclude that our numerical model for concrete expansion due AAR is working properly when dealing with applied loading and can be used in the study of reinforced concrete, as will be shown next.

4.2 Evaluation of reinforcement

In this example, we are testing the behavior of plain and reinforced concrete, based on the experimental measurements developed by [33], in order to validate the present numerical model. The specimens consist of plain and reinforced prisms of 225 x 225 x 400 mm, with 360 days of measurements. One prism was reinforced with four grade 60 no. 3 deformed bars, 25 mm away from corners, along the greater dimension.

The following properties were adopted for concrete: Young's modulus of 20 GPa, asymptotic volumetric strain (ε_{vol}^{max}) of 0.0046, reactivity index (A_1) of 750.0 days, porous filling time (t^p) of 115 days. The following properties were adopted for reinforcement bars: Young's modulus of 210 GPa, yield strength of 433 MPa, Ø9.525 mm (3/8 in).

Once again, since the specimens were kept sealed in water at 38°C, the calibration variables related to moisture and porosity (k_m and k_p) were assumed equal unity (no influence). The calibration variable related to temperature (k_t) was set equal to 0.2, like the last example. The calibration variable related to stress state (k_c) was set equal to 0.0001 (almost no expansion when limit achieved). In this example, we adopted a limit of -5MPa as boundary for the stress linear normalization law.

The numerical and experimental results are presented in Fig. 4. The numerical expansion is reduced as expected, but the results do not match. That means that the presented model is able to evaluated reinforced concrete structures under expansion due AAR, but the effect of AAR on the bond characteristics must be improved, following recent researches [34].

Besides, as a benchmark example, we replaced the rebars by the same tax of steel fibers (0.56%), randomly distributed on the concrete matrix, leading to 4839 steel fibers of length 30 mm and diameter 1 mm.

Fig 5 shows the spatial distribution of the steel fibers, as well the discretization of the specimen into 314 tetrahedral elements and 1878 nodes, also used in plain and reinforced concrete. The numerical expansion has been already presented in Fig. 4. The expansion of specimen with steel fibers is reduced as expected, yet leading to smaller expansion that the reinforced specimen.

5 CONCLUSIONS

A parametric model for the analysis of reinforced concrete structures subjected to expansion due alkali-aggregate reaction employing a general FEM formulation able to consider fibers spread inside the matrix has been proposed and successfully tested. The greatest advantage of the presented formulation is that inclusion of fibers (rebars) does not increase the number of degree of freedom to the system.

Its performance was first evaluated by simulating AAR expansion in a cylinder, under different loading conditions. The results showed the accuracy with the laboratory assessment behaviour. Afterwards, a reinforced concrete prism was modeled. Although the numerical results do not match the experimental measurements, they show the expected behaviour – reduction in the expansion in the rebars direction. We propose that the effect of AAR on the bond characteristics must be evaluated to improve results. An extension has also been provided, employing steel fiber elements randomly distributed in the concrete matrix.

Since the formulation was able to solve the presented problems, we plan to extend its features to cover debounding processes as well as concrete damage.

6 ACKNOWLEDGEMENTS

Authors thank the National Council for Scientific and Technological Development (CNPq – 444321/2014-4) for the financial support.

7 REFERENCES

[1] Pan, JW, Feng, YT, Wang, JT, Sun, QC, Zhang, CH and Owen, DRJ (2012): Modeling of alkali-silica reaction in concrete: a review. Frontiers of structural and civil engineering (6): 1-18.

[2] Saouma, VE, Martin, RA, Hariri-Ardebili, MA and Katayama, T (2015): A mathematical model for the kinetics of the alkali-silica chemical reaction. Cement and concrete research (68): 184-195.

[3] Svensson, SE (1991): Eigenstresses generated by diffusion in a spherical particle embedded in an elastic medium. International journal of mechanical sciences (33): 211-223.

[4] Bazant, ZP and Steffens, A (2000): Mathematical model for kinetics of alkali-silica reaction in concrete. Cement and concrete research (30): 419-428.

[5] Poyet, S, et al. (2007): Chemical modelling of alkali silica reaction: influence of the reactive aggregate size distribution. Materials and structures (40): 229-239.

[6] Oberholster, RE (1983): Alkali reactivity of silicious rock aggregates: diagnosis of the reaction testing of cement and aggregate and prescription of preventive measures. In: 6th International Conference on Alkalis in Concrete, June, 1983, Copenhagen, Denmark: 419-433.

[7] Capra, B and Bournazel, JP (1998): Modeling of induced mechanical effects of alkali aggregate reactions. Cement and concrete research (28): 251-260.

[8] Carey, G, Fowkes, N, Staelens, A and Pardhanani, A (2004): A class of coupled nonlinear reaction diffusion models exhibiting fingering. Journal of computational and applied mathematics (166): 87-99.
[9] Ulm, FJ, Coussy, O, Kefei, L and Larive, C (2000): Thermo-chemo-mechanics of ASR expansion in concrete structures. Journal of engineering mechanics (126): 233-242.
[10] Comi, C, Fedele, R and Perego, U (2009): A chemo-thermo-damage model for the analysis of concrete dams affected by alkali-silica reaction. Mechanics of materials (41): 210-230.
[11] Farage, MCR, Alves, JLD and Fairbairn, EMR (2004): Macroscopic model of concrete subjected to alkali-aggregate reaction. Cement and concrete research (34): 495-505.
[12] Fairbairn, EMR, Ribeiro, FLB, Lopes, LE, Toledo Filho, RD and Silvoso, MM (2006): Modelling the structural behavior of a dam affected by alkali-silica reaction. Communications in numerical methods in engineering (22): 1-12.
[13] Léger, P, Coté, P and Tinawi, R (1996): Finite element analysis of concrete swelling due to alkali-aggregate reaction in dams. Computers and structures (60): 601-611.
[14] Pappalardo Jr, A, Pauletti, RMO and Pimenta PM (2000): Numerical simulation of the alkali-aggregate reaction in concrete dams – in Portuguese. Revista Mackenzie de engenharia e computação (1): 181-199.
[15] Carrazedo, R and Lacerda, LA (2008): Parametric model for the analysis of concrete expansion due to alkali aggregate reaction. Journal of strain analysis for engineering design (43): 325-335.
[16] Pietruszczak, S (1996): On the mechanical behaviour of concrete subjected to alkali-aggregate reaction. Computers and structures (58): 1093-1097.
[17] Kagimoto, H, Yasuda, Y and Kawamura, M (2014): ASR expansion, expansive pressure and cracking in concrete prisms under various degrees of restraint. Cement and concrete research (59): 1-15.
[18] Multon, S and Toutlemonde, F (2006): Effect of applied stresses on alkali-silica reaction-induced expansions. Cement and concrete research (36): 912-920.
[19] Vanalli, L, Paccola, RR and Coda, HB (2008): A simple way to introduce fibers into FEM models. Communication in numerical methods in engineering (24): 585-603.
[20] Sampaio, MSM, Paccola, RR and Coda, HB (2013): Fully adherent fiber-matrix FEM formulation for geometrically nonlinear 2D solid analysis. Finite elements in analysis and design (66): 12-25.
[21] Paccola, RR, Piedade Neto, D and Coda, HB (2015): Geometrical non-linear analysis of fiber reinforced elastic solids considering debounding. Composite Structures (133): 343-357.
[22] Coda, HB (2009): A solid-like FEM for geometrically non-linear 3D frames. Computer methods in applied mechanics and engineering (198): 3712-3722.
[23] Coda, HB and Paccola, RR (2008): A positional FEM formulation for geometrical non-linear analysis of shells. Latin American journal of solids and structures (5): 205-223.
[24] Ciarlet, PG (1993): Mathematical elasticity: three-dimensional elasticity. North-Holland: pp. 451.
[25] Larive, C (1998): Apports combines de l'experimentation et de la modélisation à la comprehension del'alcali-réaction et de ses effets mécaniques. Laboratoire central des ponts et Chaussées, Paris.
[26] Multon, S and Toutlemonde, F (2010): Effect of moisture conditions and transfers on alkali silica reaction damaged structures. Cement and concrete research (40): 924-934.
[27] Multon, S and Toutlemonde, F (2006): Effect of applied stresses on alkali-silica reaction-induced expansions. Cement and concrete research (36): 912-920.
[28] Carrazedo, R, Sanches, RAK and Lacerda, LA (2012): Numerical modeling of orthotropic concrete expansion due alkali-aggregate reaction by a parametric model. In: 10h World Congress on Computational Mechanics, June 2012, São Paulo, Brazil.
[29] Ogden, RW (1984): Non-linear elastic deformations. England, Ellis Horwood: pp. 560.
[30] Paccola, RR, Sampaio, MSM and Coda, HB (2015): Fiber-matrix contact stress analysis for elastic 2D composite solids. Latin American journal of solids and structures (12): 583-611.
[31] Sampaio, MSM, Paccola, RR and Coda, HB (2015): A geometrically nonlinear FEM formulation for the analysis of fiber reinforced laminated plates and shells. Composite structures (119): 799-814.
[32] Carles-Gibergues, A and Cyr, M (2002): Interpretation of expansion curves of concrete subjected to accelerated alkali-aggregate reaction (AAR) tests. Cement and Concrete Research (32): 691-700.

[33] Fan, S and Hanson, JM (1998): Length expansion and cracking of plain and reinforced concrete prisms due to alkali-silica reaction. ACI Materials Journal (95): 480-487.
[34] Beglariage, A and Yazici, H (2013): The effect of alkali-silica reaction on steel fiber-matrix bond characteristics of cement based mortars. Construction and Building Materials (47): 845-860.

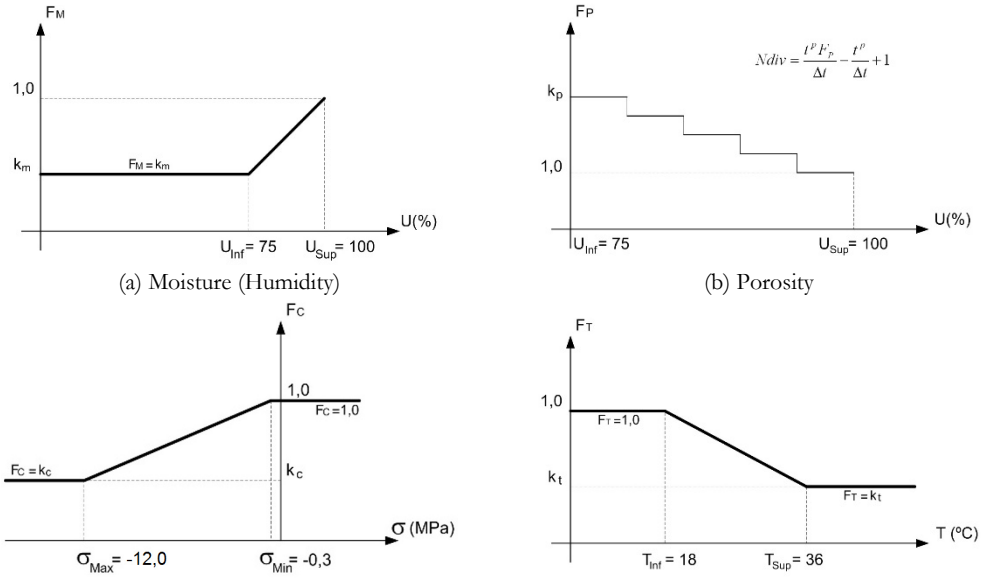

(a) Moisture (Humidity) (b) Porosity

(c) Principal Stress Component / Confinement (d) Temperature

FIGURE 1: Influence Factors and Calibration Variables.

Source: (a), (c) and (d) [14], (b) [15]

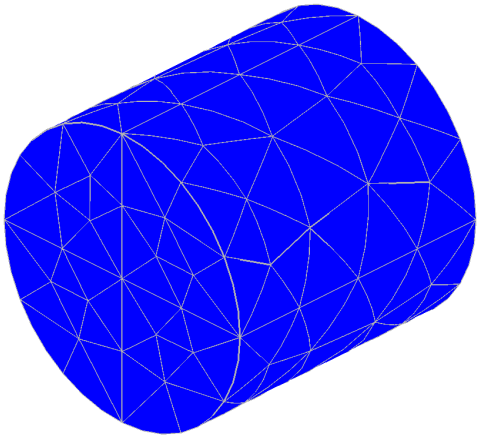

FIGURE 2: Finite element discretization of whole cylindrical specimen.

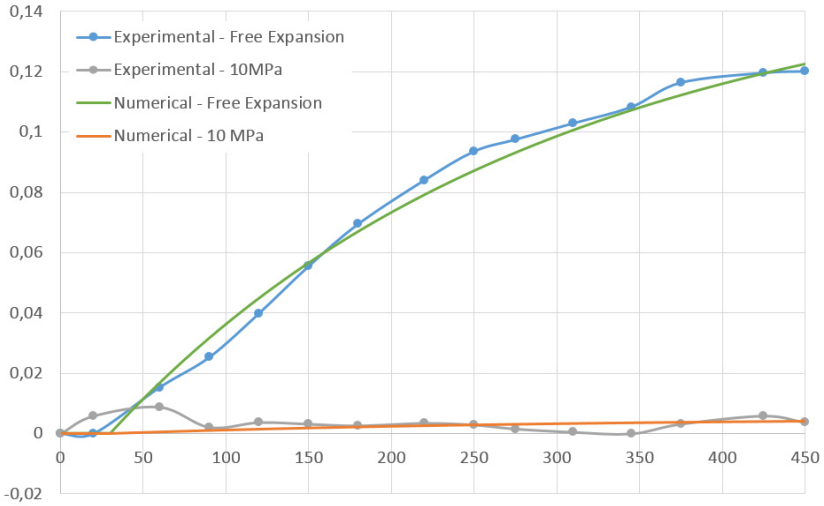

FIGURE 3: Axial strains due to AAR of mortar specimen under different loading conditions.

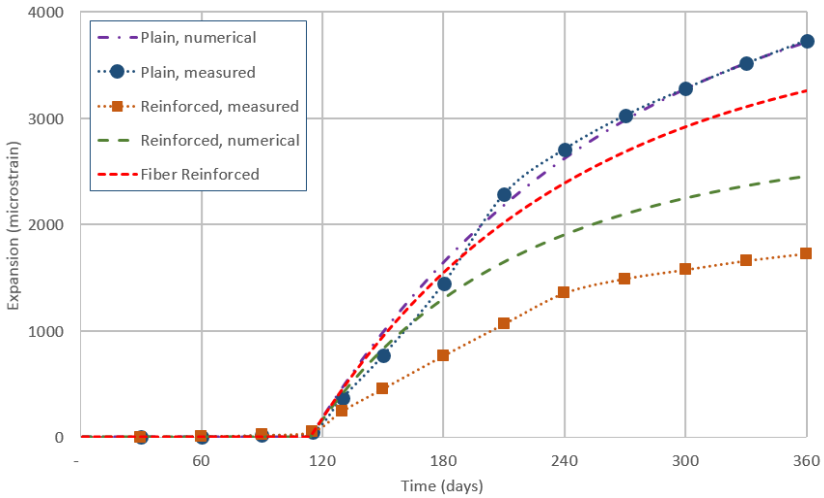

FIGURE 4: Axial strain of plain and reinforced concrete prism.

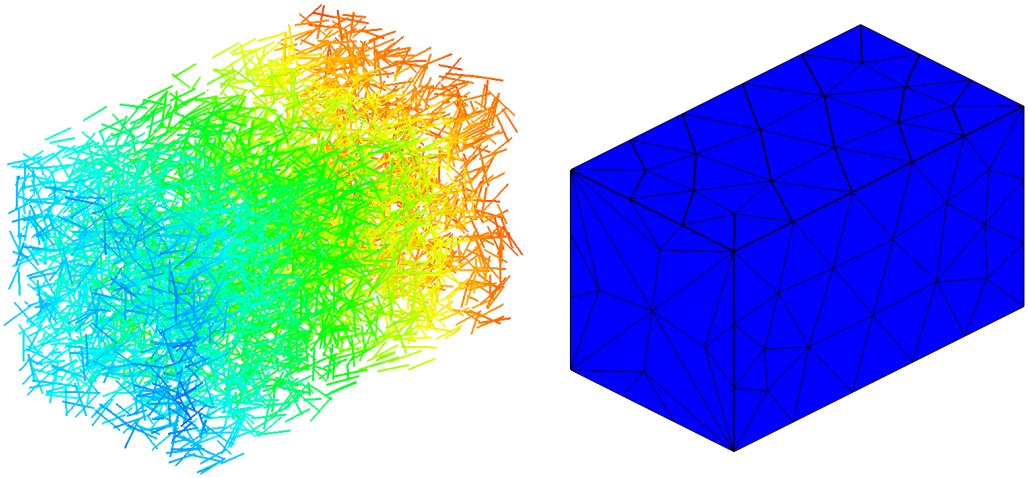

(a) Steel Fibers (b) Concrete matrix

FIGURE 5: Finite element discretization of prismatic specimen with steel fibers.